State control of phonon collision in a spherical Bose-Einstein condensate

Tianyou Gao[1,6], Jian-Song Pan[3], Dongfang Zhang[1], Lingran Kong[1,6], Ruizong Li[1,6], Xing Shen[1,6], Xiaolong Chen[4], Shi-Guo Peng[1], Mingsheng Zhan[1,5], W. Vincent Liu[2,3,5],* and Kaijun Jiang[1,5]†

[1] *State Key Laboratory of Magnetic Resonance and Atomic and Molecular Physics, Wuhan Institute of Physics and Mathematics, Chinese Academy of Sciences, Wuhan, 430071, China*

[2] *Department of Physics and Astronomy, University of Pittsburgh, Pittsburgh, Pennsylvania 15260, USA*

[3] *Wilczek Quantum Center, School of Physics and Astronomy and T. D. Lee Institute, Shanghai Jiao Tong University, Shanghai 200240, China*

[4] *Centre for Quantum and Optical Science, Swinburne University of Technology, Melbourne 3122, Australia*

[5] *Center for Cold Atom Physics,Chinese Academy of Sciences, Wuhan, 430071, China and*

[6] *School of Physics, University of Chinese Academy of Sciences, Beijing 100049, China*

(Dated: May 15, 2018)

The control of collective excitations and collision between them provides a forefront for understanding non-equlibrium many-body dynamics. Ultracold atomic gases with a tunability are excellent for conducting such a new quantum control [1–3]. Previous experiments were performed mostly in anisotropic traps due to technical challenges [4–9]. Consequently, the energy spectra of excitation modes are densely distributed with less or no well-defined symmetry, which makes it difficult to accurately manipulate coherent excitations. Here we produce a spherical Rb Bose-Einstein condensate (BEC) in an optical dipole trap and observe the phonon parametric down-conversion (PPDC). The conversion process shows that a high-energy mode is coupled to a low-energy mode with a half eigen-frequency [10, 11]. The spherical symmetry, which is crucial for observing the PPDC, is experimentally verified by measuring the collective modes and expansion behaviors of the condensate.

The study of elementary excitations is an important task of quantum many-body theories. In the case of Bose fluids, in particular, it plays a crucial role in the understanding of the properties of superfluid liquid helium and was the subject of pioneering works by Landau, Bogoliubov, and Feynman [12–14]. There has been an intensive study of the excitations in quantum Bose and Fermi gases [4–9]. But all the previous researches are limited to the anisotropic trap due to technical challenge, where the angular momentum is not a good quantum number and different excitations are not well separated from each other due to the breaking of the SO(3) rotational symmetry. The dense excitation spectra make the accurate control of collective modes as well as comparison between theory and experiment difficult. Recently Lobster *et al.* studied the low-lying excitations of a high-temperature Bose gases in a spherical magnetic trap, where the quantum fluctuation is unimportant [15, 16]. The study and control of elementary excitations of an isotropic pure quantum gas is still lacked.

In this letter, we produce a spherical Rb BEC in an optical dipole trap. We find that the monopole mode can be produced through coupling with a high-energy mode with a twice eigen-frequency, in a manner analogous to the parametric down-conversion of light in a nonlinear media [11]. This process can be called the phonon parametric down-conversion (PPDC). The underling mechanism of the PPDC is the collisions between phonons. The well-defined symmetries of the Bogoliubov modes of a spherical BEC prevent a lot of uncontrollable coupling by the conservation laws, which makes the observation of a high-order PDC process possible. The unique properties of the spherical condensate: the expansion behaviors predicted by analytical theory, and the eigen-frequencies and decaying rates of the collective modes predicted by the Bogoliubov perturbation theory, are all experimentally verified.

Parametric down-conversion (PDC) of photons in nonlinear crystal has been widely used to produce high-qualified correlated photon pairs in quantum techniques [11], while the lack of strong interaction between photons limits the proliferation of entanglement. By contrast, our discovery provide a possibility for the application of phonons, whose interaction can be tuned by using a magnetic field or optical field, in future quantum techniques. It is worth noting that the PPDC observed here originates from the high-order expansion of the inter-particle interaction. While seeming available in predicting the parametric up-conversion, the mean-field theory is qualitatively incorrect in describing the PPDC process [17]. Our reported observation therefore opens the challenge in related theoretical study to advance beyond mean-field theory.

We produce a spherical ^{87}Rb BEC in an optical dipole trap in which the trapping frequencies along the $x, y, z-$directions are the same. The experimental setup is shown in Fig.1(a). The spherical trap is composed of the dipole trap and the gravity. We produce a pure spherical ^{87}Rb BEC by accurately adjusting the relative position and intensity of the two beams in the last stage of the evaporation cooling. By measuring the oscillation of the center of the mass (COM) of the atomic cloud in the trap, we get the trapping frequencies: $\omega_x = 2\pi \times 76.7$

* wvliu@pitt.edu

† kjjiang@wipm.ac.cn; Tianyou Gao, Jian-Song Pan and Dongfang Zhang contributed equally to this work

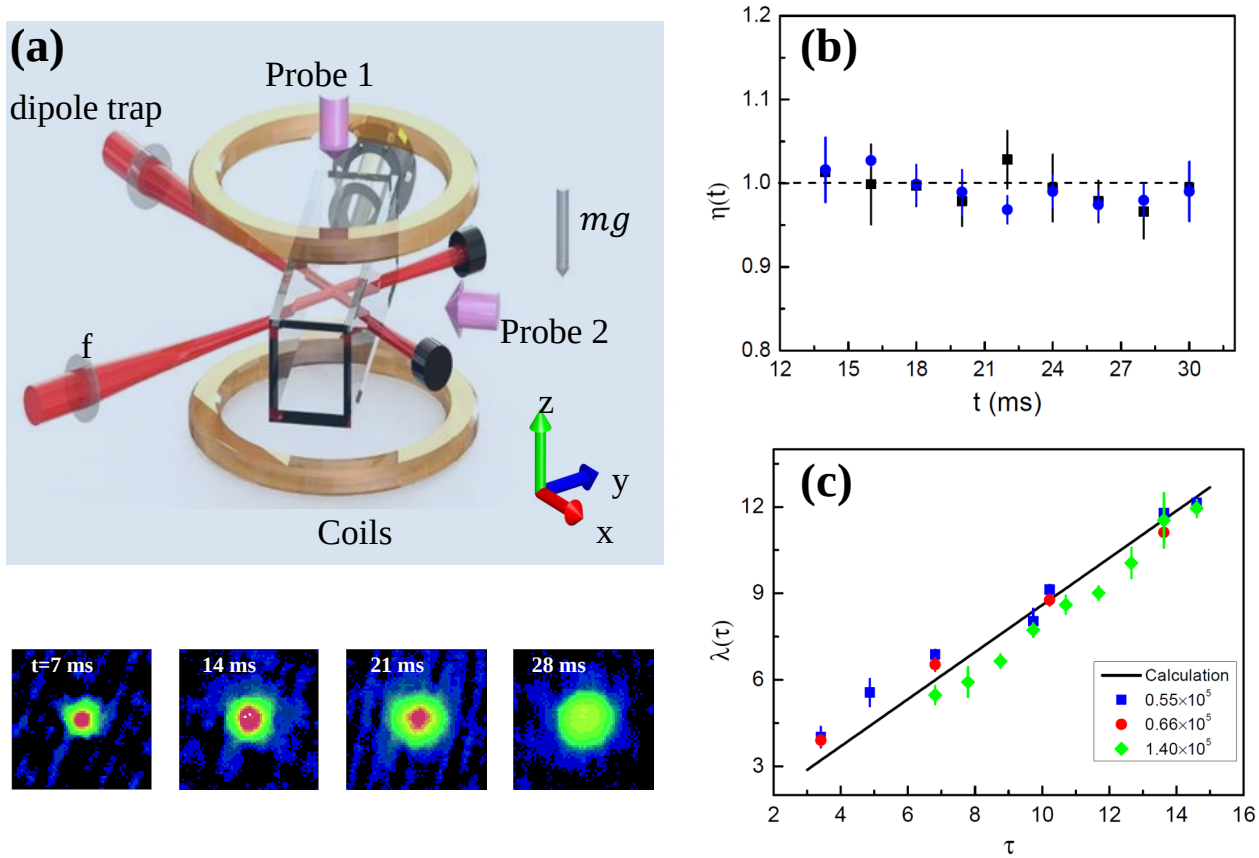

FIG. 1. (color online) Forming a spherical Rb BEC. (a) Experimental setup. Two focused red-detuned laser beams propagate along x and y directions, respectively. The gravity is along the $-z$ direction. Ultracold atoms are simultaneously probed in the vertical and horizontal directions. Spherical atomic clouds are shown with free expansion time t = 7 ms, 14 ms, 21 ms, 28 ms. (b) Aspect ratio $\eta(t)$ versus the free expansion time t. The black squares (blue circles) are fo the images probed in the horizontal (vertical) direction. The error bars indicate the uncertainties for three measurements. (c) The scaled BEC width $\lambda(\tau) = R(\tau)/R(0)$ versus τ. $R(0)$ is the initial Thomas Fermi radius of BEC in the trap and $\tau = \omega_0 t$. Blue squares, red circles and green diamonds are for atom numbers of 0.55×10^5, 0.66×10^5 and 1.40×10^5. The black solid curve is the calculation of Eq.(1).

Hz, $\omega_y = 2\pi \times 76.5$ Hz, $\omega_z = 2\pi \times 79.4$ Hz. So the mean trapping frequency $\bar{\omega} = (\omega_x + \omega_y + \omega_z)/3 = 2\pi \times 77.5$ Hz which is much larger than that in the reference [15]. The tight confinement here is favorite to produce a pure Bose condensate and obtain experimental data with a high signal-to-noise ratio. The asphericity $A = (\omega_{max} - \omega_{min})/\bar{\omega} \approx 3.7\%$, where ω_{max}, ω_{min} are the maximum and minimum trapping frequencies along three directions, respectively. It is required that the position stability of the dipole beam should be better than 3 μm to maintain the BEC a good spherical shape (see Supplementary Information). The atoms stay in the spin state $|F, m_F >= |1, -1 >$. The atomic temperature is 80(10) nK from analyzing the free expansion of the small fraction of the thermal gases co-existing with the condensate, and the atom number of BEC is $1.2(1) \times 10^5$.

The aspect ratio $\eta(t)$ of the condensate during the free expansion is probed in Fig.1(b) by suddenly switching off the optical trap. For the images probed along the horizontal direction, $\eta(t) = R_{xy}(t)/R_z(t)$ where $R_{xy}(t)$ and $R_z(t)$ are the Thomas-Fermi radius in the horizontal and vertical directions, respectively. For the images probed from the vertical direction, $\eta(t) = R_x(t)/R_y(t)$ where $R_x(t)$ and $R_y(t)$ are the Thomas-Fermi radius in the x and y directions, respectively. $\eta(t)$ remains unity during the free expansion, which indicates the unique isotropic expansion for a spherical BEC. The free expansion of an anisotropic BEC is anisotropic, in which the aspect ratio $\eta(t)$ approaches an asymptotic value dependent on the ratio of the trapping frequencies [3, 18, 19].

Analytically solving the expansion of an anisotropic BEC is difficult because it needs to solve three or two coupled second-order differential equations [3, 20, 21]. While the free expansion of a spherical BEC can be analytically solved because it only needs to solve one second-order

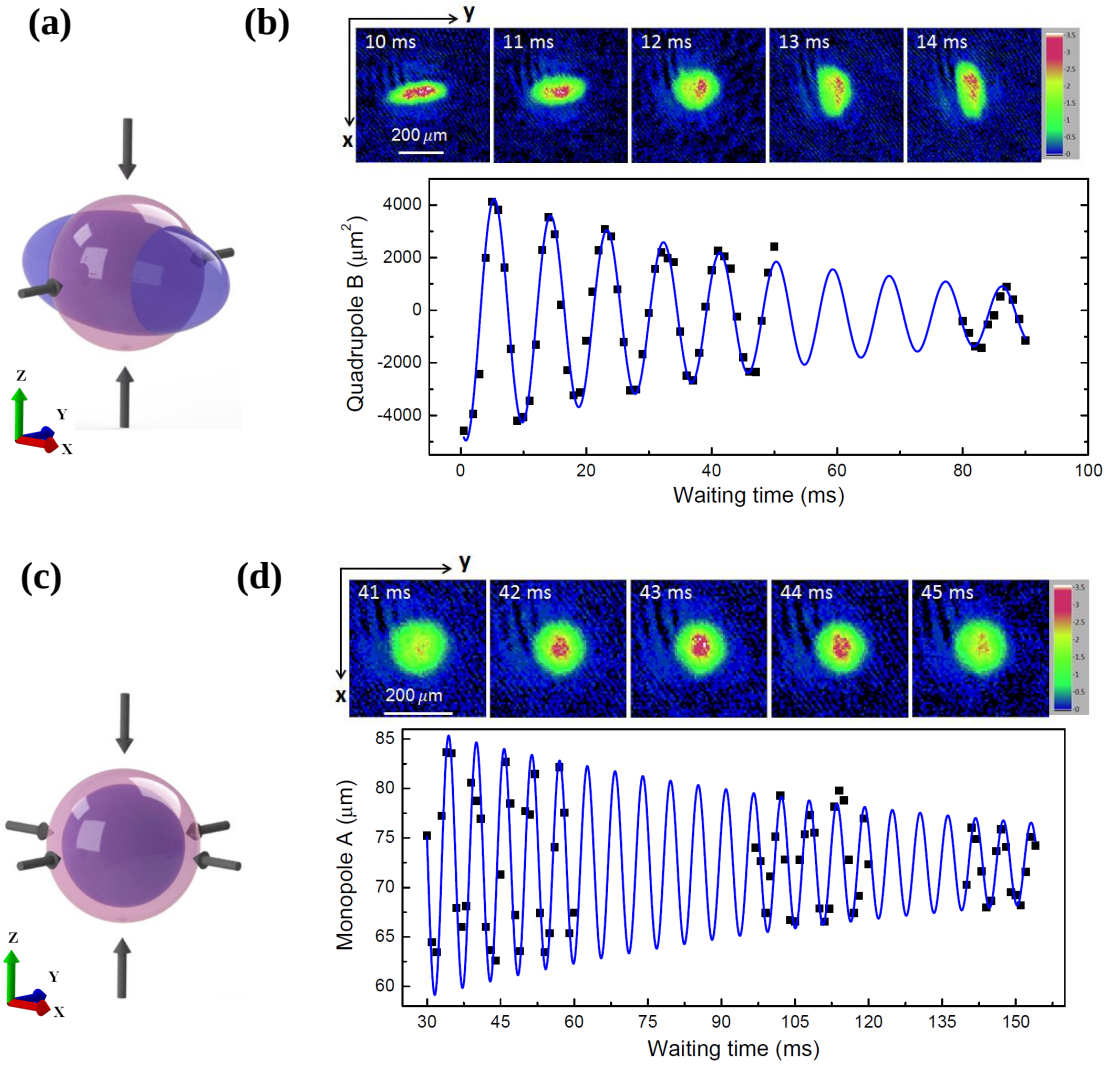

FIG. 2. (color online) Collective modes of a spherical BEC. (a) Schematics of driving the quadrupole mode. The condensate is compressed and decompressed simultaneously in y and z directions, and then it oscillates out of phase between the $y-z$ plane and the x direction. (b) Oscillation of the quadrupole mode. The upper row shows atom clouds probed for the waiting time of 10 ms, 11 ms, 12 ms, 13 ms and 14 ms in the trap. The lower row shows the oscillation of the parameter $B = R_x^2 - R_y^2$. The blue solid curve is the numerical fitting with a damped sinusoidal function. (c) Schematics of driving the monopole mode. The condensate is compressed and decompressed simultaneously in x, y and z directions, and then it oscillates in phase in three directions. (d) Oscillation of the monopole mode. The upper row shows atom clouds for the waiting time of 41 ms, 42 ms, 43 ms, 44 ms and 45 ms in the trap. The lower row shows the oscillation of the effective width $A = \sqrt{R_x^2 + R_y^2 + R_z^2}$. The blue solid curve is the numerical fitting with a damped sinusoidal function.

differential equation $\frac{\partial^2 \lambda}{\partial \tau^2} = \lambda^{-4}$, whose solution is

$$\tau = -\sqrt{\frac{3}{2}} \cdot \frac{\sqrt{\pi}\Gamma(2/3)}{\Gamma(1/6)} + \sqrt{\frac{3}{2}}\lambda \cdot {}_2F_1(-\frac{1}{3}, \frac{1}{2}, \frac{2}{3}, \frac{1}{\lambda^3}) \quad (1)$$

where $\tau = \omega_0 t$ with the trapping frequency ω_0, $\lambda(t) = R(t)/R(0)$, where $R(0)$ is the initial Thomas-Fermi radius of the BEC in the trap and can be calculated with the atomic number and the trapping frequency. $\Gamma(\cdot)$ is the Gamma function, and ${}_2F_1(\cdot)$ is the hypergeometric function. Due to the limited resolution of our imaging system ($\Delta r \approx 7.6$ μm) [22], we only show the experimental data for expansion time larger than 7 ms in the Fig.1(c). Experimental results with three atomic numbers all have good agreements with the theoretical calculation of Eq. (1).

Collective excitations are the crucial elements of low energy quantum dynamics and response functions in interacting many-body systems. We will study two elementary collective modes, the monopole and quadrupole mode. In an anisotropic trap, these two modes cou-

ple each other even under the zero-order approximation. Consequently, only the coupled and less-symmetric modes can be experimentally accessible [4–9]. In a spherical trap, the two modes are decoupled and we can study each specific mode individually. While the frequencies of these two modes are close, a specific mode can be selectively excited according to its symmetry. The modulation lasts ten periods and then the condensate is probed for different waiting time in the trap, using the absorption-imaging method with a time of flight (TOF) of 28 ms.

We first excite the quadrupole mode by modulating the intensity of the beam along the x direction with a frequency of about $\sqrt{2}\omega_0$. As shown in Fig.2(a), the condensate is compressed and decompressed simultaneously in y and z directions, and then it oscillates out of phase between the $y-z$ plane and the x direction. The modulation amplitude $\delta\omega_{y0}/\omega_{y0}$ along y direction is about 12%. We show atom clouds probed for five different waiting time in the trap on the upper row of Fig.2(b). We consider images probed from the vertical direction and analyze the relative changes between x and y directions. The condensate size can be extracted by fitting the atomic image with a Thomas-Fermi distribution. We define a parameter $B = R_x^2 - R_y^2$ to quantitatively describe the quadrupole mode, where $R_i (i = x, y)$ is the Thomas-Fermi radius of the condensate. As shown in Fig.2(b), the experimental data are fitted using the damped sinusoidal function $B_0 + \delta B \exp(-t/t_0)\sin(\omega_Q t)$. From the fitting, $\omega_Q = 2\pi \times 111.21(32)$ Hz $= 1.435(4)\omega_0$, which is consistent with the value $\sqrt{2}\omega_0$ calculated for the spherical Bose condensate [23]. The lifetime of the quadrupole mode is $t_0 = 58.2(66)$ ms, which is also consistent to the calculation for the spherical condensate (see Methods). The statistics errors come from the uncertainty in the fitting process.

Then we excite the monopole mode with a spherical symmetry by simultaneously modulating the intensities of the two trapping beams. When the driving frequency ω_p equals to the eigen-frequency of the monopole mode, the atom loss is serious due to the deformation of the trapping potential (see Supplementary Information). While we *surprisingly* find the monopole mode can only be excited when the driving frequency ω_p is about twice of the eigen-frequency. As shown in Fig.2(c), the variations of the two beams are accurately balanced so that the condensate keeps nearly a sphere when oscillating in the trap. The modulation amplitude $\delta\omega_0/\omega_0$ is about 10%, where $\delta\omega_0$ is the variation of the trapping frequency during the modulation. The condensate is compressed and decompressed simultaneously in x, y and z directions, and then it oscillates in phase in three directions after the modulation being stopped. The upper row of the Fig.2(d) shows atom clouds for five different waiting time in the trap. We define an effective width $A = \sqrt{R_x^2 + R_y^2 + R_z^2}$ to quantitatively study the monopole oscillation. As shown in Fig.2(d), we numerically fit the experimental data using a damped sinusoidal function $A_0 + \delta A \exp(-t/t_0)\sin(\omega_M t)$. From the fitting, $\omega_M = 2\pi \times 176.93(31)$ Hz $= 2.283(4)\omega_0$, which is consistent with the value $\sqrt{5}\omega_0$ calculated for the spherical Bose condensate [23]. The lifetime of the monopole mode is $t_0 = 104.4(57)$ ms, which is also consistent to the calculation for the spherical condensate (see Methods).

Here the driving frequency $\omega_p \approx 2\pi \times 340$ Hz is about twice the eigen-frequency of the monopole mode and nearly resonant with the mode $(n, l) = (2, 1)$. The coupling mechanism between mode $(n, l) = (2, 1)$ and monopole mode can be explained as PPDC in Fig. 3(a). For convenience, we call the monopole as mode 1, the mode $(n, l) = (2, 1)$ as mode 2 and the stationary Bose condensate as mode 0. Expanding the interaction term up to the second-order with respect to the fluctuation above the ground state is the central idea to calculate collective modes in the Bogoliubov theory. The third-order expansion gives rise to the coupling between the collective modes. In an ideal spherical trapping potential, parity symmetry forbids the coupling of mode $(2, 1)$ to the monopole mode. While here the gravitational force makes the isotropic potential slightly deformed and develops an odd parity in the z-direction. The first-order term is absorbed by the shift of the trap center, then we only consider the third-order deformation $V' = \lambda z^3$ of the trap. The deformation is weak and a perturbation analysis is applicable. The coefficient characterizing the probability of the down-conversion process is given by [17, 24]

$$\begin{aligned} M_{12} =& 2\int d\boldsymbol{r}\psi_0'[(2\tilde{u}_1^*\tilde{v}_1^* + \tilde{u}_1^*\tilde{u}_1^*)\,\tilde{u}_2 \\ &+ (2\tilde{u}_1^*\tilde{v}_1^* + \tilde{v}_1^*\tilde{v}_1^*)\,\tilde{v}_2], \end{aligned} \tag{2}$$

where $\begin{pmatrix} \tilde{u}_\nu & \tilde{v}_\nu \end{pmatrix} = \begin{pmatrix} u_\nu' & v_\nu' \end{pmatrix} - c_\nu \begin{pmatrix} \psi_0' & -\psi_0'^* \end{pmatrix}$ with $c_\nu = \int d\boldsymbol{r}\psi_0' u_\nu' \approx -\int d\boldsymbol{r}\psi_0' v_\nu'$ is the orthogonalized collective mode wave function with respect to the ground-state wave function. The prime denotes the normalized perturbed wave functions.

The PPDC process is described by the Lagrangian $\mathcal{L} = i\hbar\sum_{j=1,2}\hat{b}_j^\dagger\partial_t\hat{b}_j + \hbar\kappa(\hat{b}_2^\dagger\hat{b}_1^2 e^{i\Delta t} + \hat{b}_1^{\dagger 2}\hat{b}_2 e^{-i\Delta t})/2$, where $\hat{b}_j$ ($\hat{b}_j^\dagger$) annihilates (creates) a phonon of mode j, $\kappa = |NgM_{12}/\hbar|$ is the coupling coefficient and $\Delta = (\omega_2' - 2\omega_1')$ with the perturbed eigen-frequency ω_j' (see Supplementary Information) [17]. In our experiment, $\lambda \approx 0.0175 a_H^{-3}$, $\Delta \approx 0.2\omega = 2\pi \times 15.50$ Hz and $\kappa \approx 0.90\omega = 2\pi \times 69.75$ Hz. The effective coupling strength for the PPDC process can be estimated as $\xi = |\beta_2\kappa|^2/\Delta \approx 3.98|\beta_2|^2\omega = 2\pi \times 308.45|\beta_2|^2$, where $\beta_2 = \langle\hat{b}_2\rangle$ is the mean-field probability amplitude of mode 2. The non-zero M_{12} indicates the parametric down-conversion is permissible by symmetry in our experiment.

Since modes 1 and 2 can couple back and forth and the total energy is conserved, the two modes can be considered as an effective mode f. The atom population transferred from the ground state 0 to state f is proportional to the total excitation energy in the driving process. The

width of the population distribution with respect to the driving frequency is proportional to the effective damping rate γ_f of state f. We find the total excitation energy finally completely flows to mode 1 through the PPDC process, such that we can experimentally measure the width by probing the monopole oscillation amplitude in the long time limit. If other damping processes are neglected, γ_f should be in the range $[\gamma_1, \gamma_2]$, where γ_1 and γ_2 are the Landau damping rates of mode 1 and mode 2, respectively. As shown in Fig. 3(b), the observed distribution of the amplitude of the monopole mode well supports the above picture. The amplitude of the monopole mode is very sensitive on the driving frequency and becomes maximum only when the mode (2,1) is resonantly excited. This demonstrates that the oscillation of the monopole mode originates from the mode (2,1) through the PDC process. Unlike the PDC of photons, where a pump phonon (Ω_p) is split as a signal photon (Ω_s) and an idle photon (Ω_i) via the optical nonlinear coupling (in general, the maximum conversion possibility locates at $\Omega_s = \Omega_i$), one high-frequency phonon (mode 2) is split as two low-frequency phonons (mode 1) by colliding with the ground-state atoms (mode 0) (see Fig. 3(a)).

In Fig. 4, we directly observe the parametric down-conversion from the mode (2,1) to the monopole mode during the mode-excitation process. Here we modulate the dipole trap for different time and then probe the position and width of the condensate without waiting time in the trap. For mode (2,1), only the center-of-mass of the atomic cloud oscillates while the size does not change (see Supplementary Information). This facilitate directly probing the two modes individually. In our trapping configuration comprising of an optical dipole trap and gravity, changing the trapping frequency simultaneously excites the center-of-mass motion along the z direction. This corresponds to the mode ($n = 2, l = 1, m = 0$) with the eigen frequency of $\sqrt{19}\omega_0$. The oscillation of the center of mass along the z direction is shown in Fig. 4(a). We use a double-sine function $z_0 + A_1 \sin(\omega_1(t - t_1)) + A_2 \sin(\omega_1(t - t_2)/\sqrt{19})$ to fit the experimental data. $\omega_1 = 2\pi \times 338.07(91)$ Hz $= 4.36(1)\omega_0$ is very close to the eigen frequency of the mode (2,1) and $\omega_1/\sqrt{19}$ close the frequency of the dipole mode. $A_1^2/A_2^2 = 2.15$ means that the population in mode (2,1) is about twice that of the dipole mode. This is reasonable because we resonantly excite the mode (2,1) while the dipole mode is excited with a far detuning. We also simultaneously probe the atomic size in Fig. 4(d). The atomic widths in x, y and z directions change without a constant phase for a short driving time, but start to oscillate in phase when the driving time is longer than 21 ms. This is the signal that the monopole mode is produced after certain time. We fit the effective width $A = \sqrt{R_x^2 + R_y^2 + R_z^2}$ with a sinusoidal function and obtain the oscillation frequency $\omega = 2\pi \times 170.13(173)$ Hz $\approx 2.20(2)\omega_0$, which is very close to the eigen frequency $\sqrt{5}\omega_0$ of the monopole mode.

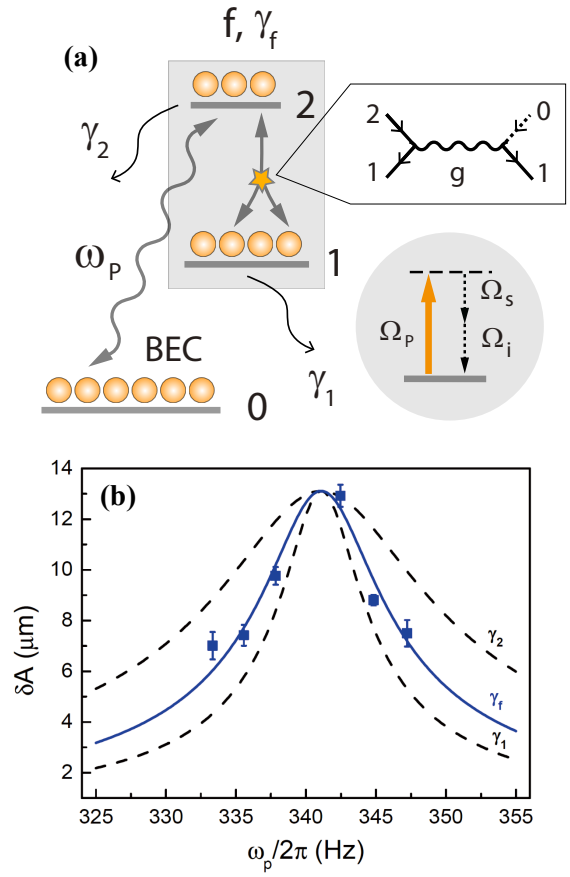

FIG. 3. (Color online) Phonon parametric down-conversion (PPDC). (a) Schematics for the driving and down-conversion processes. Bose condensate (mode 0) is excited with a frequency ω_p to the mode 2 ($(n = 2, l = 1)$). Mode 2 and mode 1 (monopole mode) are coupled by the interaction. As illustrated by the Feynman diagram in the open pentagon, one phonon 2 and one phonon 0 merge as two phonons 1. The coupled two modes can be considered as one effective mode f. $\gamma_{i=1,2,f}$ denote the damping rates of the mode i. As a comparison the PDC of photons is shown in the rounded shadow box. (b) Oscillation amplitude δA of the monopole mode versus ω_p. The blue squares are the experimental data and the error bars denote the uncertainties in fitting the oscillation of the monopole mode as in Fig. 2(d). The blue solid curve is the numerical fitting with a Lorentz function, giving $\gamma_f = 2\pi \times 2.01$ Hz. Two dashed curves are the Lorentz distributions with widths of $\gamma_1 = 2\pi \times 1.36$ Hz and $\gamma_2 = 2\pi \times 3.57$ Hz given by the numerical calculation. The heights are normalized by the experimental data.

While the nonlinear coupling between collective modes has been reported in an anisotropic BEC [25, 26], the possibility that the observed phenomenon is a PDC process has been excluded later [17]. More precisely, considering the enhancement of the trapping potential, the PPDC observed here resembles more like the cavity-enhanced PDC [27] than that in free space. The observed Beliaev damping in the homogenous limit [28] is substantially dif-

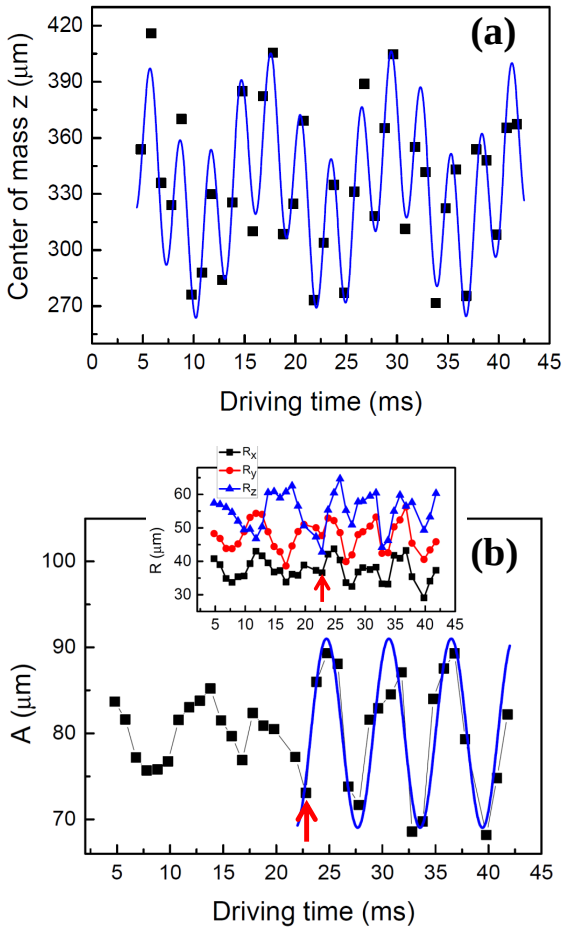

FIG. 4. (Color online) Probing PPDC in the driving process. (a) The center of mass of the atomic cloud along the z direction versus the excitation time. The experimental data are fitted with a double-sine function. The obtained two oscillation frequencies, $1.01\omega_0$ and $4.36\omega_0$, correspond to the dipole mode and the mode (2,1), respectively. (b) Observation of the monopole mode. When the driving time is bigger than 21 ms (indicated by the red arrow), the condensate widths in x, y and z directions begin to oscillate in phase (see the inset), indicating the produced monopole mode. We fit the effective width$A = \sqrt{R_x^2 + R_y^2 + R_z^2}$ with a sinusoidal function and get the oscillation frequency $\omega = 2\pi \times 170.65(1.61)$ Hz $\approx 2.21(1)\omega_0$.

ferent from the PPDC observed here. On one hand, the modes participating in the PPDC are all the eigen-modes of the interacting Hamiltonian with a long lifetime. The modes involved in the Beliaev damping is the Fourier plane waves that are not the eigenstates of the Bogoliubov Hamiltonian. On the other hand, unlike the PPDC process observed here, the Beliaev damping is inherently irreversible due to the continuous spectrum. Our study is a pioneering work for the state control of the collective excitation, which is expected to stimulate further experimental and theoretical studies in understanding non-equlibrium many-body dynamics.

Methods

Forming spherical condensate. To form a spherical trap, we use the combination of the optical dipole trap and the gravity. The setup is the improvement of our previous experiment [29]. As shown in Fig.1(a), the two dipole beams propagate along x and y directions and the gravity is in the $-z$ direction. The combined trap is given by

$$\begin{aligned} U(x,y,z) = &-U_1 \exp\left(-\frac{2x^2}{w_{1x}^2} - \frac{2z^2}{w_{1z}^2}\right) \\ &- U_2 \exp\left(-\frac{2y^2}{w_{2y}^2} - \frac{2z^2}{w_{2z}^2}\right) - mgz. \end{aligned} \tag{3}$$

If neglecting the gravity term in the Eq.(3), it should satisfy the condition $w_{1x}^2/w_{1z}^2 + w_{2y}^2/w_{2z}^2 = 1$ to form a spherical BEC should. w_{1x} and w_{1z} are the waists of the laser beam along the y direction, and w_{2y} and w_{2z} for the beam along the x direction. In the experiment, it is scarcely possible to accurately match a specific relation by modulating the relative shapes of beams. Fortunately, the gravity force can soften this strict condition. Considering the gravity force in Eq.(3), the condition will change to $U_1/w_{1x}^2 = U_2/w_{2y}^2$, where U_1 and U_2 are the peak potentials of the two beams, respectively. In this case, we can accurately adjust the relative intensities of the two beams to form a spherical BEC. In our experiment, $w_{1x} \approx w_{2y} \approx 65$ μm and $w_{1z} \approx w_{2z} \approx 68$ μm. Forming a good spherical BEC requires that the positions of two dipole beams can be adjusted with a high accuracy and stability. We use the combination of one AOM and one PZT-driven mirror to adjust the position of one dipole beam. The position accuracy and stability can reach 3 μm. We always calibrate the trapping frequencies to keep the asphericity $A < 5\%$ when measuring collective modes.

Driving mode ($n = 2, l = 1$) without destroying the spherical symmetry. In order to drive mode ($n = 2, l = 1$) without destroying the spherical symmetry, we simultaneously modulate the intensities of the two trapping beams, i.e. $I_i(t) = I_{i0} + \delta I_{i0} \sin \omega_p t$ ($i = 1, 2$). The modulation frequency of the two beams is about $\sqrt{19}\omega_0$ which is the eigen frequency of mode ($n = 2, l = 1$). I_{i0} is the initial optical intensity. The variations δI_{i0}(i=1, 2) of the two beams are accurately balanced so that the condensate remains nearly a sphere when oscillating in the trap. In our trapping configuration, the potential minimum along the z direction is given by $z_0 = \frac{mg}{4(U_1/w_{1z}^2 + U_2/w_{2z}^2)}$. Changing the optical intensities excites the center of mass along the z direction, such that the mode ($n = 2, l = 1, m = 0$) is excited.

Probing atoms. The population in the spin state $|F, m_F >= |1, -1>$ is pumped to the spin state $|F >=$

$|2>$ before being resonantly probed with a TOF of 28 ms. The atoms are simultaneously probed in vertical and horizontal directions, respectively, to get the widths along three directions. The probe light has a weak power of 50 μW and a short pulse of 50 μs. In this case the probing in one direction has negligible effect on the probing in the other direction.

Calculating the Landau damping rate. Landau damping, in which low-energy collective mode is absorbed in the transition between thermal excitations, is dominant at finite temperature [30, 31]. We calculate the Landau damping of the collective modes based on the perturbation theory developed by Pitaevskii *et al.* [30, 32, 33]. Accordingly the damping rate is calculated with the expression,

$$\gamma = \left(\pi/\hbar^2\right) \sum_{ik} \left|A_{ik}\right|^2 \delta\left(\omega_{ik} - \Omega_{osc}\right)\left(f_i - f_k\right), \qquad (4)$$

where $f_\nu = \left[\exp\left(E_\nu/k_B T\right) - 1\right]^{-1}$ is the thermal occupation of mode $\nu = i, k$ with the temperature T and Boltzmann constant k_B, Ω_{osc} is the eigenfrequency of the oscillation mode, $\omega_{ik} = \omega_i - \omega_k$ is the frequency difference, and $\delta(.)$ is the Dirac function. Here $A_{ik} = 2g \int d\boldsymbol{r} \psi_0 [(u_k^* \upsilon_i + \upsilon_k^* \upsilon_i + u_k^* u_i) u_{osc} + (\upsilon_k^* u_i + \upsilon_k^* \upsilon_i + u_k^* u_i) \upsilon_{osc}]$ is the transition amplitude of a specific damping channel, where g is the interaction strength, $(\psi_0, -\psi_0^*)$ and $(u_\nu, \upsilon_\nu)^T$ are the wave functions of the zero-energy Nambu-Goldstone mode and the ν-th collective mode, respectively (see Supplementary Information). The lifetime of the collective mode is given by $\tau = 1/\gamma$. In general, due to the uncertainties like the imperfection of the trapping potential and the finite lifetime of the collective mode, the energy level has a finite width. We need to replace the δ-function with a Lorentz distribution with the width Δ, i.e. $\delta(\omega_{ik} - \Omega_{osc}) \to \Delta/(2\pi\hbar)[(\omega_{ik} - \Omega_{osc})^2 + \Delta^2/4]$. In fact, γ is unsensitive with Δ when it is far larger than the average level space and smaller than Ω_{osc}. The calculated lifetime for the monopole and quadrupole modes are about 111.9 ms and 49.3 ms, respectively, which show good agreement with the experimental measurements.

Acknowledgments

We acknowledge fruitful discussions with Gora Shlyapnikov, David Papoular, and Shizhong Zhang. This work has been supported by the NKRDP (National Key Research and Development Program) under Grant No. 2016YFA0301503, NSFC (Grant No. 11474315, 11674358, 11434015) and CAS under Grant No. YJKYYQ20170025. J.-S. P. acknowledges support from National Postdoctoral Program for Innovative Talents of China under Grant No. BX201700156.

[1] Griffin, A. *Excitations in a Bose-Condensed liquid* (Cambridge University Press, New York, 1993).

[2] Bloch, I., Dalibard, J. & Zwerger, W. Many-body physics with ultracold gases. *Rev. Mod. Phys.* **80**, 885–964 (2008).

[3] Dalfovo, F., Giorgini, S., Pitaevskii, L. P. & Stringari, S. Theory of Bose-Einstein condensation in trapped gases. *Rev. Mod. Phys.* **71**, 463–512 (1999).

[4] Jin, D. S., Ensher, J. R., Matthews, M. R., Wieman, C. E. & Cornell, E. A. Collective excitations of a Bose-Einstein condensate in a dilute gas. *Phys. Rev. Lett.* **77**, 420–423 (1996).

[5] Mewes, M.-O. *et al.* Collective excitations of a Bose-Einstein condensate in a magnetic trap. *Phys. Rev. Lett.* **77**, 988–991 (1996).

[6] Chevy, F., Bretin, V., Rosenbusch, P., Madison, K. W. & Dalibard, J. Transverse breathing mode of an elongated Bose-Einstein condensate. *Phys. Rev. Lett.* **88**, 250402 (2002).

[7] Kinast, J., Hemmer, S. L., Gehm, M. E., Turlapov, A. & Thomas, J. E. Evidence for superfluidity in a resonantly interacting Fermi gas. *Phys. Rev. Lett.* **92**, 150402 (2004).

[8] Altmeyer, A. *et al.* Precision measurements of collective oscillations in the BEC-BCS crossover. *Phys. Rev. Lett.* **98**, 040401 (2007).

[9] Nascimbene, S. *et al.* Collective oscillations of an imbalanced Fermi gas: Axial compression modes and polaron effective mass. *Phys. Rev. Lett.* **103**, 170402 (2009).

[10] Armstrong, J. A., Bloembergen, N., Ducuing, J. & Pershan, P. S. Interactions between light waves in a nonlinear dielectric. *Phys. Rev.* **127**, 1918–1939 (1962).

[11] Giallorenzi, T. G. & Tang, C. L. Quantum theory of spontaneous parametric scattering of intense light. *Phys. Rev.* **166**, 225–233 (1968).

[12] Landau, L. D. The theory of superfluidity of helium ii. *J. Phys. (USSR)* **5**, 71 (1941).

[13] Bogoliubov, N. N. On the theory of superfluidity. *J. Phys. (USSR)* **11**, 23–32 (1947).

[14] Feynman, R. P. Progress in low temperature physics. *edited by C. J. Gorter (North-Holland, Amsterdam, 1955)* **1**, 17.

[15] Lobser, D. S., Barentine, A. E. S., Cornell, E. A. & Lewandowski, H. J. Observation of a persistent non-equilibrium state in cold atoms. *Nat. Physics* **11**, 1009–1013 (2015).

[16] Straatsma, C. J. E. *et al.* Collapse and revival of the monopole mode of a degenerate bose gas in an isotropic harmonic trap. *Phys. Rev. A* **94**, 043640 (2016).

[17] Hechenblaikner, G., Morgan, S. A., Hodby, E., Maragò, O. M. & Foot, C. J. Calculation of mode coupling for quadrupole excitations in a Bose-Einstein condenstate. *Phys. Rev. A* **65**, 033612 (2002).

[18] Ernst, U., Marte, A., Schreck, F., Schuster, J. & Rempe, G. Bose-einstein condensation in a pure Ioffe-Pritchard field configuration. *Europhys. Lett.* **41**, 1–6 (1998).

[19] Stamper-Kurn, D. M. *et al.* Optical confinement of a Bose-Einstein condensate. *Phys. Rev. Lett.* **80**, 2027–

2030 (1998).
[20] Castin, Y. & Dum, R. Bose-einstein condensates in time dependent traps. *Phys. Rev. Lett.* **77**, 5315–5319 (1996).
[21] Baym, G. & Pethick, C. J. Ground-state properties of magnetically trapped Bose-condensed rubidium gas. *Phys. Rev. Lett.* **76**, 6–9 (1996).
[22] Gao, T., Zhang, D., Kong, L., Li, R. & Jiang, K. Optimizing the optical imaging system by *in-situ* imaging the plugged hole in ultracold atoms. *arXiv:* 1708.03988v1 (2017).
[23] Stringari, S. Collective excitations of a trapped Bose-condensed gas. *Phys. Rev. Lett.* **77**, 2360–2363 (1996).
[24] Morgan, S., Choi, S., Burnett, K. & Edwards, M. Nonlinear mixing of quasiparticles in an inhomogeneous bose condensate. *Phys. Rev. A* **57**, 3818 (1998).
[25] Hechenblaikner, G. *et al.* Observation of harmonic generation and nonlinear coupling in the collective dynamics of a Bose-Einstein condensate. *Phys. Rev. Lett.* **85**, 692–695 (2000).
[26] Hodby, E., Maragò, O. M., Hechenblaikner, G. & Foot, C. J. Experimental observation of Beliaev coupling in a Bose-Einstein condensate. *Phys. Rev. Lett.* **86**, 2196–2199 (2001).
[27] Ou, Z. & Lu, Y. Cavity enhanced spontaneous parametric down-conversion for the prolongation of correlation time between conjugate photons. *Phys. Rev. Lett.* **83**, 2556 (1999).
[28] Katz, N., Steinhauer, J., Ozeri, R. & Davidson, N. Beliaev damping of quasiparticles in a Bose-Einstein condensate. *Phys. Rev. Lett.* **89**, 220401 (2002).
[29] Zhang, D., Gao, T., Kong, L., Li, K. & Jiang, K. Production of rubidium Bose-Einstein condensate in an optically plugged magnetic quadrupole trap. *Chin. Phys. Lett.* **33**, 076701 (2016).
[30] Pitaevskii, L. & Stringari, S. Landau damping in dilute Bose gases. *Phys. Lett. A* **235**, 398 – 402 (1997).
[31] Dalfovo, F., Minniti, C. & Pitaevskii, L. P. Frequency shift and mode coupling in the nonlinear dynamics of a Bose-condensed gas. *Phys. Rev. A* **56**, 4855–4863 (1997).
[32] Fedichev, P. O., Shlyapnikov, G. V. & Walraven, J. T. M. Damping of low-energy excitations of a trapped Bose-Einstein condensate at finite temperatures. *Phys. Rev. Lett.* **80**, 2269–2272 (1998).
[33] Guilleumas, M. & Pitaevskii, L. P. Temperature-induced resonances and landau damping of collective modes in Bose-Einstein condensed gases in spherical traps. *Phys. Rev. A* **61**, 013602 (1999).

SUPPLEMENTARY INFORMATION

Manipulating the optical dipole trap

Forming a good spherical BEC requires that the positions of two dipole beams can be adjusted with a high accuracy and stability. We use the combination of one acousto-optic modulator (AOM) and one PZT-driven mirror to adjust the position of one dipole beam as shown in Fig. S 5. The temperature shift of the AOM has a big effect on the beam spatial stability. To solve this problem, we use a flipped mirror to reflect away the dipole beam during the laser cooling and evaporation cooling in the magnetic trap, and then open the optical dipole beam for loading atoms. The AOM is only switched off for about 100 ms in which we probe atoms with a time of flight. In this way the AOM keeps working for most time in the experimental period of about 40 seconds and the temperature change is less than 0.5 ^{0}C. The dipole beam position can be adjusted with an accuracy of about 1 μm. The position stability of the dipole beam is better than 3 μm.

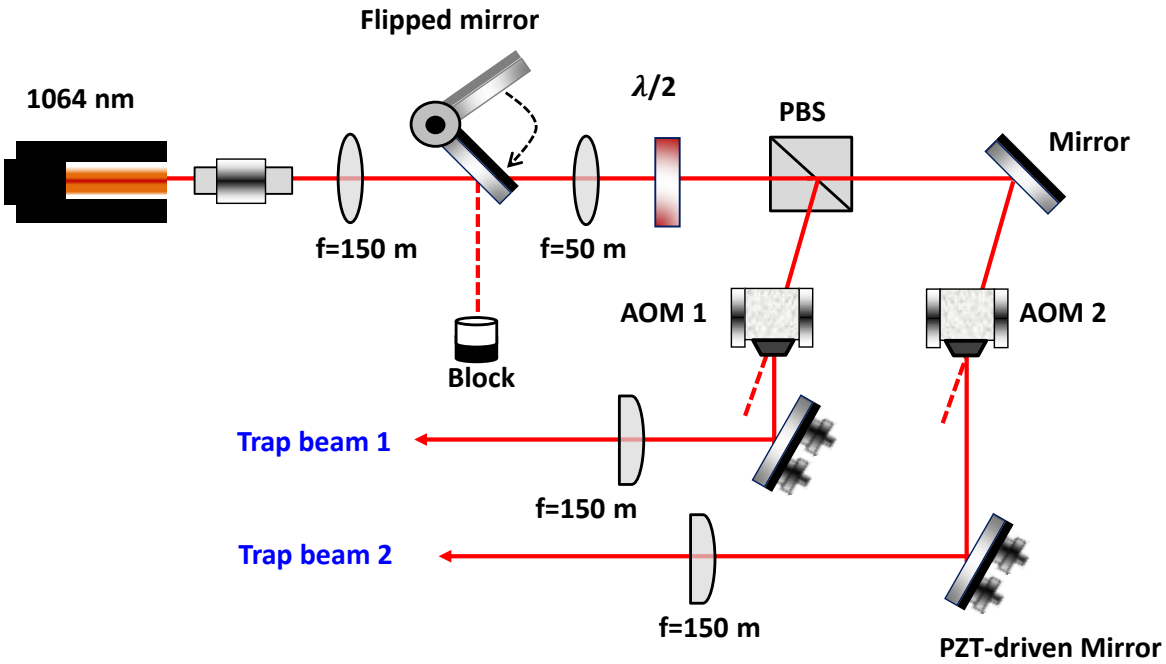

FIG. 5. (color online) Schematics for the two dipole beams of the spherical trap. Two trap beams come from the one IPG laser with a wavelength of 1064 nm. One acousto-optic modulator (AOM) and one PZT-driven mirror are used together to accurately adjust the position of one dipole beam with a high repeatability. The flipped mirror can reflect the dipole beams, making the AOM open most of the time. PBS: polarization beam splitter. $\lambda/2$: half-wave plate

Atom loss in the spherical modulation

As mentioned in the main text, the gravity force helps us in forming a spherical Bose-Einstein condensate (BEC). But on the other hand, it will tilt the potential along the $-z$ direction as shown in Fig. S 6 (a). In the driving process with spherical symmetry, atoms have a tendency to escape from the trap along the $-z$ direction. We find that there is no atom loss with small modulation amplitude $\delta\omega_0/\omega_0 < 5\%$, while the monopole mode couldn't be observed when $\delta\omega_0/\omega_0 < 8\%$. In the experiment, we choose $\delta\omega_0/\omega_0 = 10\%$, and in this condition the atom loss versus the modulation frequency is shown in Fig. S 6 (b). It is shown that the atom loss is serious when the modulation frequency equals to the eigen frequency of the monopole mode.

We numerically simulate the dynamics of the BEC with a non-interacting Hamiltonian for simplicity:

$$H = -\frac{\hbar^2}{2m}\nabla^2 + \left\{-U_1 \exp\left(-\frac{2x^2}{w_{1x}^2} - \frac{2z^2}{w_{1z}^2}\right) - U_2 \exp\left(-\frac{2y^2}{w_{2y}^2} - \frac{2z^2}{w_{2z}^2}\right)\right\}\left[1 + \alpha \sin\left(\omega_p t\right)\right] - mgz. \tag{5}$$

$\alpha = 10\%$ is the modulation amplitude. Both the numerical simulation and experimental results show that the atom loss is big for slow modulation and small for fast modulation. When the modulation frequency $\omega_p \geq 3\omega_0$, the remained atom number roughly equals to the initial value. We finally observe the PPDC when $\omega_p \approx 2\pi \times 340$ Hz $= 4.39\omega_0$, where the atoms loss is negligibly small.

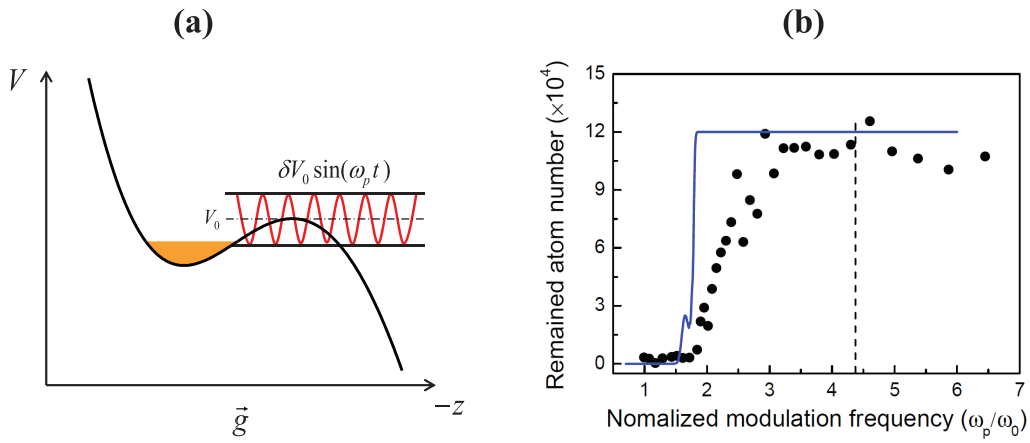

FIG. 6. (color online) Atom loss in the spherical modulation. (a) Modulation of the trap potential. The gravity force ($\vec{g}$) is along the $-z$ direction. The trap potential is modulated with a sinusoidal function $\delta V_0 \sin(\omega_p t)$. (b) The remained atom in the trap versus the normalized modulation frequency (ω_p/ω_0). The black solid circles are the measured atom numbers. The blue solid curve is the calculation based on the calculation based on Eq.(5) single-particle model. The vertical dashed line indicates the modulation frequency to observe PPDC, $\omega_p = 2\pi \times 340$ Hz $\approx 4.39\omega_0$, where the atoms loss is negligibly small

Bogoliubov spectrum of a spherical condensate

The Hamiltonian of our system can be written as

$$H = \int d^3\boldsymbol{r}\hat{\psi}^\dagger \left(-\frac{\hbar^2}{2m}\nabla^2 + V(\boldsymbol{r}) + \frac{g}{2}\hat{\psi}^\dagger\hat{\psi}\right)\hat{\psi}, \tag{6}$$

where $\hat{\psi}$ is the field operator of the bosons, $V(\boldsymbol{r}) = \frac{1}{2}m\omega^2 r^2$ is the trapping potential with the trapping frequency ω and $g = 4\pi\hbar^2 a_s/m$ with the scattering length a_s is the interaction coefficient. In our experiment, $\omega \approx 2\pi \times 77.5$ Hz and the characteristic length of the trapping potential $a_H = \sqrt{\hbar/m\omega} \approx 1.24\mu m$. Obviously, this Hamiltonian possesses the $SO(3)$ rotation symmetry and $U(1)$ gauge symmetry.

The dynamics of the BEC can be described by the Gross-Pitaevskii (GP) equation[1–3]

$$i\hbar\frac{\partial\psi}{\partial t} = \left(-\frac{\hbar^2}{2m}\nabla^2 + V(\boldsymbol{r}) + g|\psi|^2\right)\psi, \tag{7}$$

where $\psi = \langle\hat{\psi}\rangle$ is the condensate wave function.

In order to find the collective modes of the BEC, we rewrite ψ as

$$\psi(\boldsymbol{r},t) = e^{-i\mu t/\hbar}\left[\psi_0(\boldsymbol{r}) + \sum_j \left(u_j(\boldsymbol{r})e^{-i\omega_j t} + \upsilon_j^*(\boldsymbol{r})e^{i\omega_j t}\right)\right], \tag{8}$$

where ψ_0 is the ground-state wave function, μ the chemical potential, u_j and υ_j the "particle" and "hole" components with eigen-frequency $\pm\omega_j$ respectively of the Bogoliubov transformations. Substituting Eq. (8) into Eq. (7), we derive the Bogoliubov-de Gennes (BdG) equation

$$\begin{pmatrix} -\frac{\hbar^2}{2m}\nabla^2 - \mu + V(\boldsymbol{r}) + 2g|\psi_0|^2 & g\psi_0^2 \\ -g\psi_0^{*2} & -\left(-\frac{\hbar^2}{2m}\nabla^2 - \mu + V(\boldsymbol{r}) + 2g|\psi_0|^2\right) \end{pmatrix}\begin{pmatrix} u_j \\ \upsilon_j \end{pmatrix} = \hbar\omega_j\begin{pmatrix} u_j \\ \upsilon_j \end{pmatrix}. \tag{9}$$

Here the ground-state wave function ψ_0 and the chemical potential μ are determined by the stationary GP equation

$$\left(-\frac{\hbar^2}{2m}\nabla^2 + V(\boldsymbol{r}) + g|\psi_0|^2\right)\psi_0 = \mu\psi_0, \tag{10}$$

and the particle number equation $N_0 = \int d^2\boldsymbol{r}\,|\psi_0|^2$, where N_0 is the ground-state particle number. Under the parameters of our experiment, since the coefficient reflecting the ratio between the interaction energy and the kinetic energy $N_0 a_s/a_H \approx 560 \gg 1$, the Thomas-Fermi approximation is applicable,

$$\psi_0 \approx \begin{cases} \left(\mu - m\omega^2 r^2\right)^{1/2} & , \quad r \leq \sqrt{\mu/m\omega^2} \\ 0 & , \quad r > \sqrt{\mu/m\omega^2} \end{cases}. \tag{11}$$

Since Hamiltonian (6) possesses the rotation symmetry, Eq. (9) can be divided into independent sectors denoted by the angular momentum quantum number (l, m), where $l = 0, 1, 2, ...$ and $m = -l, -l-1, ...l$ are the quantum numbers arising from the total angular momentum and the z-component of the angular momentum respectively. Under the spherical coordinate system $\boldsymbol{r} = (r, \theta, \phi)$, we expand (u_j, υ_j) as

$$\begin{pmatrix} u_j(\boldsymbol{r}) \\ \upsilon_j(\boldsymbol{r}) \end{pmatrix} = \sum_{lm} \begin{pmatrix} u_j^{(lm)}(r) \\ \upsilon_j^{(lm)}(r) \end{pmatrix} Y_{lm}(\theta, \phi), \tag{12}$$

where $Y_{lm}(\theta, \phi)$ is the spherical harmonic wave function. Substituting Eq. (12) into Eq. (9) and integrating the two sides with $\int_0^{2\pi} d\phi \int_0^{\pi} d\theta Y_{lm}(\theta, \phi) \sin\theta$, we derive

$$\begin{pmatrix} h_0(r) + 2g|\psi_0|^2 & g\psi_0^2 \\ -g\psi_0^{*2} & -\left(h_0(r) + 2g|\psi_0|^2\right) \end{pmatrix} \begin{pmatrix} u_j^{(lm)}(r) \\ \upsilon_j^{(lm)}(r) \end{pmatrix} = \hbar\omega_j^{(lm)} \begin{pmatrix} u_j^{(lm)}(r) \\ \upsilon_j^{(lm)}(r) \end{pmatrix}, \tag{13}$$

where $h_0(r) = -\frac{\hbar^2}{2m}\left[\frac{1}{r^2}\frac{d}{dr}\left(r^2\frac{d}{dr}\right) - \frac{l(l+1)}{r^2}\right] + V(r)$. The above equation is solved numerically. Since the transformation $\{(\ u_j\ \ \upsilon_j\ ), \hbar\omega_j\} \longrightarrow \{(\ \upsilon_j^*\ \ u_j^*\ ), -\hbar\omega_j\}$ doesn't change Eq. (9), one can get the wave functions of the "hole" component by looking at the wave function of the "particle" component. For convenience, we sort the non-negative eigen-energy from small to large and denote it with integer j from 0 to infinity for each sector (l, m). The lowest excited collective mode with spherical symmetry, mode $(n, l) = (1, 0)$, is called monopole mode, while the lowest excited mode with $l = 1$, mode $(0, 1)$ and that with $l = 2$, mode $(0, 2)$, are respectively called dipole mode and quadrupole mode.

For convenience, we use the Dirac brackets $|\psi_j\rangle$ with the eigen-energy E_j to denote the j-th zero-order collective mode (i.e. $\langle\boldsymbol{r}|\psi_j\rangle = (\ u_j\ \ \upsilon_j\ )^T$, $E_j = \hbar\omega_j$). The zero-energy Goldstone mode $(\psi_0, -\psi_0^*)^\dagger$ is denoted with $|\psi_0\rangle$. The orthogonality of the collective modes can be given by

$$\langle\psi_i|\sigma_z|\psi_j\rangle = \int d\boldsymbol{r}\,(u_i^* u_j - \upsilon_i^* \upsilon_j) = \mathrm{sign}(\omega_j)\,\delta_{ij}. \tag{14}$$

According to the Riesz-Schauder theory, the subspace expanded by $|\psi_0\rangle$ is incomplete [4, 5]. To construct a complete eigenspace, one need to introduce the complementary mode $\langle\boldsymbol{r}|\phi_0\rangle = (\ \phi_0(\boldsymbol{r})\ \ \phi_0^*(\boldsymbol{r})\ )^T$ through the equation [6–9]

$$\sigma L_0|\phi_0\rangle = \alpha|\psi_0\rangle, \tag{15}$$

where the zero-order Bogoliubov Hamiltonian,

$$L_0 = \begin{pmatrix} -\frac{\hbar^2}{2m}\nabla^2 - \mu + V(\boldsymbol{r}) + 2g|\psi_0|^2 & g\psi_0^2 \\ g\psi_0^{*2} & -\frac{\hbar^2}{2m}\nabla^2 - \mu + V(\boldsymbol{r}) + 2g|\psi_0|^2 \end{pmatrix}. \tag{16}$$

Here the constant α is selected to make

$$\langle\psi_j|\sigma_z|\phi_0\rangle = \int d\boldsymbol{r}\left(u_j^*(\boldsymbol{r})\,\phi_0(\boldsymbol{r}) - \upsilon_j^*(\boldsymbol{r})\,\phi_0^*(\boldsymbol{r})\right) = \delta_{j0}. \tag{17}$$

The completeness of the eigenspace is given by [6–9]

$$\sum_{j\neq 0} \mathrm{sign}(\omega_j)\,|\psi_j\rangle\langle\psi_j| + |\phi_0\rangle\langle\psi_0| + |\psi_0\rangle\langle\phi_0| = I\sigma_z, \tag{18}$$

where I is the unit operator.

The monopole mode (1,0) and the collective mode (2,1) of a spherical condensate

In the above section, we analyze the collective modes in a statistic system. If the system is perturbed by some time-dependent modulation, the collective modes may be excited and the BEC will oscillate with the frequencies of the collective modes. We can measure the oscillation with some observables like the width or the center-of-mass position of the BEC. The corresponding relation between the oscillation forms and excited modes will be discussed in this subsection.

Generally, the oscillating BEC can be described by the normalized wave function

$$\psi\left(\boldsymbol{r},t\right)=e^{-i\mu t/\hbar}\left[b_0\left(t\right)\psi_0\left(\boldsymbol{r}\right)+\sum_{\omega_j>0}\left(b_j\left(t\right)u_j\left(\boldsymbol{r}\right)e^{-i\omega_j t}+b_j^*\left(t\right)\upsilon_j^*\left(\boldsymbol{r}\right)e^{i\omega_j t}\right)\right], \tag{19}$$

where the coefficients satisfy $\left|b_0\left(t\right)\right|^2+\sum_j\left|b_j\left(t\right)\right|^2=N$. When the excited atom number $\sum_j\left|b_j\left(t\right)\right|^2$ is small, the expectation of any observable $\hat{A}$ can be expanded as

$$\langle\hat{A}\rangle\left(t\right)=\left|b_0\left(t\right)\right|^2\langle\hat{A}\rangle_0+2b_0\left(t\right)\left|b_j\left(t\right)\right|\sum_{\omega_j>0}\left|\langle\hat{A}\rangle_{0j}\right|\cos\left(\omega_j t+\theta\right), \tag{20}$$

where $\langle\hat{A}\rangle_0=\int d\boldsymbol{r}\psi_0^*\left(\boldsymbol{r}\right)\hat{A}\psi_0\left(\boldsymbol{r}\right)$, $\langle\hat{A}\rangle_{0j}=\int d\boldsymbol{r}\psi_0^*\left(\boldsymbol{r}\right)\hat{A}\left(u_j\left(\boldsymbol{r}\right)+\upsilon_j^*\left(\boldsymbol{r}\right)\right)$, and θ is a relative phase.

For the monopole mode $j\rightarrow(n,l)=(1,0)$, due to the rotational symmetry of both the ground state and the monopole mode, $\langle x^2\rangle_{0j}=\langle y^2\rangle_{0j}=\langle z^2\rangle_{0j}$ and $\langle x\rangle_{0j}=\langle y\rangle_{0j}=\langle z\rangle_{0j}=0$. In general, the variation speeds of the coefficients $b_0(t)$ and $b_j(t)$ are far slower than $\cos(\omega_j t)$. Hence, the excitation of the momopole mode will lead to the periodic oscillation of the BEC width with a frequency $\omega_{mon}\approx\sqrt{5}\omega$. While for the mode $j\rightarrow(n,l,m)=(2,1,0)$, $\langle x^2\rangle_{0j}=\langle y^2\rangle_{0j}=\langle z^2\rangle_{0j}=0$, $\langle x\rangle_{0j}=\langle y\rangle_{0j}=0$, but $\langle z\rangle_{0j}\neq0$, only the z-direction center-of-mass (CoM) position oscillates with the frequency $\omega_{(2,1)}\approx\sqrt{19}\omega$ when mode $(2,1)$ is excited. Modes $j\rightarrow(n,l,m)=(2,1,\pm1)$ are not involved in a coherent driving process due to the conservation of magnetic angular momentum. This analysis constructs the base for the fitting of experimental data in the main text.

Perturbation of gravity potential

Gravity potential will make the isotropic potential deform and develop odd parity in the z-direction. The odd-parity component of the total potential $\delta V=\lambda z^3$ will couple the monopole mode with the mode $(n,l)=(2,1)$ through processes like the parametric-down conversion of photons in quantum optics. Since the deformation is weak, a perturbation analysis is applicable.

At first, the deformation will change the ground-state wave function and the chemical potential. Under the Thomas-Fermi approximation[10], the new ground-state wave function $\psi_0^{'}$ and chemical potential $\mu^{'}$ satisfy the equations $g|\psi_0^{'}|^2=\mu^{'}-V^{'}(\boldsymbol{r})$ and $\int d\boldsymbol{r}|\psi_0^{'}|^2=N_0$, where $V^{'}=V\left(\boldsymbol{r}\right)+\delta V\left(\boldsymbol{r}\right)$.

Our purpose is to derive the perturbation of the collective-mode wave functions. Since the new ground-state wave function $\psi_0^{'}$ can be gauged to be real and positive, the total perturbation term for L_0 can be written as $\delta L_0\approx(\delta\mu-\delta V)(\begin{array}{cc}1&1\end{array})^T(\begin{array}{cc}1&1\end{array})$ when $(\mu^{'}-V^{'}(\boldsymbol{r}))>0$ and $\delta L_0\approx-(\delta\mu-\delta V)I_2$ elsewhere. Here $\delta\mu=\mu^{'}-\mu$ and I_2 is the two by two identity matrix. The perturbation expansion of the BdG Eq. (16) can be written as

$$\left(L_0+\delta L_0\right)\left(|\psi_j^{(0)}\rangle+|\psi_j^{(1)}\rangle+\cdots\right)=\left(E_j^{(0)}+E_j^{(1)}+\cdots\right)\left(|\psi_j^{(0)}\rangle+|\psi_j^{(1)}\rangle+\cdots\right), \tag{21}$$

where $|\psi_j^{(n)}\rangle$ ($|\psi_j^{(0)}\rangle=|\psi_j\rangle$) and $E_j^{(n)}$ ($E_j^{(0)}=E_j$) are the n-th-order wave function and eigen-energy. The first-three-orders equation are respectively given by

$$\sigma_z L_0|\psi_j^{(0)}\rangle=E_j^{(0)}|\psi_j^{(0)}\rangle, \tag{22}$$

$$\sigma_z L_0|\psi_j^{(1)}\rangle+\sigma_z\delta L_0|\psi_j^{(0)}\rangle=E_j^{(0)}|\psi_j^{(1)}\rangle+E_j^{(1)}|\psi_j^{(0)}\rangle, \tag{23}$$

and

$$\sigma_z L_0|\psi_j^{(2)}\rangle+\sigma_z\delta L_0|\psi_j^{(1)}\rangle=E_j^{(0)}|\psi_j^{(2)}\rangle+E_j^{(1)}|\psi_j^{(1)}\rangle+E_j^{(2)}|\psi_j^{(0)}\rangle. \tag{24}$$

Integrating the two sides of Eq. (23) with $\langle\psi_j^{(0)}|\sigma_z$ and $\langle\phi_0^{(0)}| = \langle\phi_0|$, and noting that $\langle\psi_j^{(0)}|L_0|\psi_{j'}^{(1)}\rangle = E_j^{(0)}\langle\psi_j^{(0)}|\sigma_z|\psi_{j'}^{(1)}\rangle$ and $\langle\phi_0^{(0)}|L_0|\psi_{j'}^{(1)}\rangle = \alpha\langle\psi_0^{(0)}|\sigma_z|\psi_{j'}^{(1)}\rangle$, we can derive

$$E_j^{(1)} = \text{sign}\,(\omega_j)\,\langle\psi_j^{(0)}|\delta L_0|\psi_j^{(0)}\rangle, \tag{25}$$

and

$$\begin{aligned}|\psi_j^{(1)}\rangle = &\sum_{j'\neq 0,j}\text{sign}\left(E_{j'}^{(0)}\right)\frac{\langle\psi_{j'}^{(0)}|\delta L_0|\psi_j^{(0)}\rangle}{E_j^{(0)}-E_{j'}^{(0)}}|\psi_{j'}^{(0)}\rangle + \frac{\langle\phi_0^{(0)}|\delta L_0|\psi_j^{(0)}\rangle}{E_j^{(0)}}|\psi_0^{(0)}\rangle \\ &+ \frac{\langle\psi_0^{(0)}|\delta L_0|\psi_j^{(0)}\rangle}{E_j^{(0)}}\left(|\phi_0^{(0)}\rangle + \frac{\alpha}{E_j^{(0)}}|\psi_0^{(0)}\rangle\right).\end{aligned} \tag{26}$$

The condition $\langle\psi_j^{(0)}|\sigma_z|\psi_j^{(1)}\rangle = 0$ and the completeness relation (18) have been used in the above derivation. The above first-order perturbation of the wave function $\langle\boldsymbol{r}|\psi_j^{(1)}\rangle = \begin{pmatrix} u_j^{(1)} & \upsilon_j^{(1)}\end{pmatrix}$ has been used in the calculation of M_{12} in the main text. Due to the odd parity of δL_0, $E_j^{(1)} = 0$. Multiplying the two sides of Eq. (24) with $\langle\psi_j^{(0)}|\sigma_z$, we can yield the second-order perturbation of the eigen-energy

$$\begin{aligned}E_j^{(2)} =&\text{sign}\left(E_j^{(0)}\right)\{\sum_{j'\neq 0,j}\text{sign}\left(E_{j'}^{(0)}\right)\frac{\left|\langle\psi_{j'}^{(0)}|\delta L_0|\psi_j^{(0)}\rangle\right|^2}{E_j^{(0)}-E_{j'}^{(0)}} + \frac{\alpha\left|\langle\psi_0^{(0)}|\delta L_0|\psi_j^{(0)}\rangle\right|^2}{E_j^{(0)2}} \\ &+ \frac{2\text{Re}(\langle\phi_0^{(0)}|\delta L_0|\psi_j^{(0)}\rangle\langle\psi_j^{(0)}|\delta L_0|\psi_0^{(0)}\rangle)}{E_j^{(0)}}\}.\end{aligned} \tag{27}$$

Therefore, the perturbed eigen-energy is given by $E_j^{'} = \hbar\omega_j^{'} = E_j + E_j^{(2)}, j \neq 0$.

[1] Gross, E. P. Structure of a quantized vortex in boson systems. *Il Nuovo Cimento (1955-1965)* **20**, 454–477 (1961).
[2] Gross, E. P. Hydrodynamics of a superfluid condensate. *Journal of Mathematical Physics* **4**, 195–207 (1963).
[3] Pitaevskii, L. Vortex lines in an imperfect bose gas. *Sov. Phys. JETP* **13**, 451–454 (1961).
[4] Zaanen, A. C. *Linear Analysis* (North-Holland Pub., Amsterdam, 1993).
[5] Ida, M. Some mathematical aspects of multiple poles in the off-shell scattering amplitude. *Progress of Theoretical Physics* **43**, 808–829 (1970).
[6] Lewenstein, M. & You, L. Quantum phase diffusion of a bose-einstein condensate. *Physical review letters* **77**, 3489 (1996).
[7] Matsumoto, H. & Sakamoto, S. Quantum phase coordinate as a zero-mode in bose-einstein condensed states. *Progress of theoretical physics* **107**, 679–688 (2002).
[8] Lundh, E. & Rammer, J. Effective-action approach to a trapped bose gas. *Physical Review A* **66**, 033607 (2002).
[9] Rammer, J. *Quantum field theory of non-equilibrium states* (Cambridge University Press, 2007).
[10] Pethick, C. J. & Smith, H. *Bose-Einstein Condensation in Dilute Gases* (Cambridge University Press, London, 2008).